Int. J. Electrochem. Sci., 12 **(2017)** 6428 – 6444, doi: 10.20964/2017.07.41

International Journal of
ELECTROCHEMICAL
SCIENCE
www.electrochemsci.org

Highly Sensitive Electrochemical Determination of Dopamine with an Overoxidized Polypyrrole Nanofiber Pencil Graphite Electrode

Ozge Koyun[1], *Hurmus Gursu*[1,2], *Semih Gorduk*[1] *and Yucel Sahin*[1,*]

[1] Department of Chemistry, Faculty of Arts & Science, Yildiz Technical University, TR34210 Istanbul, Turkey;
[2] HMY Chemistry & Energy Ltd. Company, TR34220 Esenler, Istanbul, Turkey;
[*]E-mail: yucelsahin06@gmail.com

Received: 5 April 2017 / *Accepted:* 8 May 2017 / *Published:* 12 June 2017

We investigated the use of an overoxidized nanofiber polypyrrole (OONfPPy) modified pencil graphite electrode (PGE) as a sensor for the determination of dopamine (DA) in this work. The performance of the modified electrode was studied using differential pulse voltammetric method. The surface of the modified electrode was characterized by an electrochemical impedance spectroscopy (EIS) and scanning electron microscope (SEM). The calculated electroactive areas of the bare electrode and $OO_{10}NfPPy_5PGE$ were found to be 4.54 x 10^{-8} cm^2 and 1.05 x 10^{-6} cm^2, respectively. The sensor ($OO_{10}NfPPy_5PGE$) showed a high selectivity to DA with a detection limit of 6.95 × 10^{-9} M (S/N=3). To demonstrate the validity of the sensor for the determination of DA, pharmaceutical and human serum samples were performed.

Keywords: Dopamine; Polypyrrole; Electropolymerization**;** Pencil Graphite Electrode; Sensor

1. INTRODUCTION

As a catecholamine, dopamine (DA) is one of the most important neurotransmitters, and is widely distributed in the human central nervous system for message transfer, serving as an antecedent of adrenaline and noradrenaline, and helping to maintain hormonal balance, as well as emotion control. Abnormally high or low DA levels may lead to several neurological disorders, such as Parkinson's disease, Alzheimer's disease, schizophrenia, and epilepsy. Thus, the highly selective and sensitive detection of DA is important [1-3]. In general, the determination of DA is achieved using a spectrophotometer [4], capillary electrophoresis [5], ion-exchange chromatography [6] and high-

performance liquid chromatography (HPLC)-mass spectrometry [7], fluorometry [8], and electrochemistry [9]. Electrochemistry have received considerable attention in DA sensing, as a result of its rapid detection, ease of operation, simplicity, cost and time effectiveness, lower detection limit, miniaturization feasibility, and reliability [10]. However, a big problem with electrochemical determination of DA is the interference of some substances (e.g., ascorbic acid (AA) and uric acid (UA)). Moreover, if high concentrations of AA co-exist with DA in the extra-cellular fluid of the central nervous system, and oxidize at a potential close to that of DA at a conventional electrode, the result is an overlapping voltammetric response [11-13]. Another problem with electrochemical determination of DA is the irreversibility behavior of DA, as well as the fact that spoiling of the electrode surface by the DA oxidation product results in poor performance of conventional electrodes. In order to improve the selectivity and sensitivity of the working electrode, a great number of modified electrodes (MEs) have been proposed to determine the content of DA. A variety of electrocatalysts, such as carbon nanotubes [10], graphene [14], metal oxide nanoparticles [15], conducting polymers [16-18], and ionic liquids [19] have been used in this respect. Although electrodes other than conducting polymers are also limited with regard to sensitivity and cost, it is essential to develop a sensitive and simple method to detect DA for ordinary analysis. For these reason, the unique electrochemical features of polymers have attracted remarkable interest in the development of electrochemical sensors for DA, via electropolymerization. Electro active substances, such as pristine and derivative pyrrole [18, 20], o-phenylenediamine [21], and o-aminophenol [22], have acted as functional monomers to non-covalently interact with DA.

Conducting polymer films have been extensively investigated with regard to application in biosensors and chemical sensors. Among the various of conducting polymers, polypyrrole (PPy) is one of the most common used for the construction of bioanalytical sensors and MEs therefore it's a good redox performance, biocompatibility, and water solubility, besides its simple of change on electrode surface and powerful absorption of some analytes. It is a great ion exchanger and separator, with the capability to create nanowires and to improve conductivity. At the same time, due to its cationic structure and the presence of amino groups, it is resistant to the interference of the solution. [23-26]. It is known that the electrochemical feature of PPy is extremely dependent on its redox states, and the overoxidation of PPy, formed at potentials that are more positive than those for reversible oxidation/reduction, has frequently seen as a contributing factor to the unwanted degradation processes, It leads to the loss of conductivity and the dedoping of the anionic molecule [27, 28]. Nevertheless, in spite of these drawbacks, overoxidized PPy (OOPPy) has been used in some electroanalytical applications [29, 30].

Carbon fiber is convenient and easily accessible material with which to form the MEs [31]. PGE has a large active electrode surface area, and is thus capable of detecting low analyte concentrations. Furthermore, disposable PGE has been used because of its high electrochemical reactivity, economical, great mechanical hardness, and wide potential window. It can be also readily miniaturized and modified [32, 33]. PGE may be an attractive trace analysis technique when combined with a more accurate and sensitive voltammetric technique such as differential pulse voltammetry (DPV).

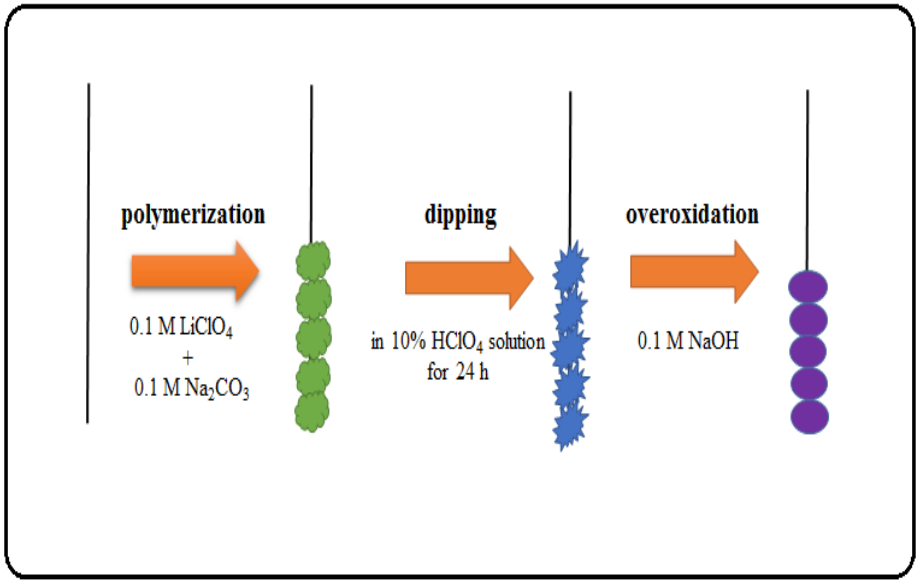

Figure 1. Schematic of the preparation process for OONfPPyPGE.

In the present study, overoxidized nanofiber polypyrrole (OONfPPy) film, using a PGE for the determination of DA, was investigated for the first time in the literature. Scheme of the preparation process of OONfPPyPGE is shown in Fig. 1. DA was selected as an analyte because of its electroactivity and popularity. However, some problems are encountered in determination of DA by electroanalytical method and these complicate the DA assay. Contamination of the polymeric structure of the electrode surface, occurring as a result of oxidation of DA, real samples to be very low concentrations of DA, oxidation peak of electroactive substances such as UA and AA located in the biological fluid to interfere with the oxidation peak of DA. A carbon-based PGE was modified to DA with nanofiber conductive polymer that has a large surface area. Also, a disposable sensor was designed by changing the surface charge of the polymer with an overoxidation process for increasing DA sensitivity. Besides, electrochemical impedance spectroscopy (EIS) was used to investigate electrode surface coating. The increase in the electroactive surface area of the working electrode was quantitatively calculated. Sensor was capable of detecting DA in the pharmaceutical and human serum samples, with satisfactory results.

2. MATERIALS AND METHODS

2.1. Reagents and apparatus

Pyrrole (Sigma Aldrich, 99% extra pure), DA hydrochloride (HCl; Sigma Aldrich), $HClO_4$ (Sigma Aldrich, 70.0-70.2%), $LiClO_4$ (Sigma Aldrich, Bioultra, > 99.0%), Na_2CO_3 (Sigma Aldrich,% 99.5- 100.5), NaOH (Sigma Aldrich, 98-100.5%), potassium phosphate dibasic (Sigma Aldrich, puriss., ≥99%), potassium phosphate monobasic (Merck), potassium hydroxide (Merck), and

phosphoric acid (Sigma Aldrich , 85%) were obtained and directly used without any purification. DA HCl purchased from a local pharmacy was used to represent real DA-containing samples. Buffer and stock solutions were prepared with deionized water in all of the electrochemical studies. Pencil leads which were purchased from a local bookstore (1.0 cm in length and 0.5 mm in diameter cm, which is Tombow of type HB) were used as a working electrode in the all electrochemical measurements, Ag/AgCl (sat. KCl) as a reference electrode, and Pt wire as a counter electrode. In the preparation of the working electrode, the electrochemical determination of DA was made by the Autolab electrochemical analyzer, model PGSTAT 302 N Potentiostat/Galvanostat. The electrochemical impedance spectrum was recorded using the Gamry 3000 model Potantiostat-Galvanostat system. All electroanalytical measurements were taken at room temperature, and pH measurements, using a HI 2211 model pH meter (Hanna Inst.), and pump gradient chromatographic measurements, using a UV-Vis detector with an HPLC system (1100 series, Agilent), were performed. Scanning electron microscopy (SEM) images were obtained using an Oxford Instruments-7430 Field Emission Electron Microscope. The weighing process was conducted using Shimadzu analytical brands (ATX224, d = 0.1 mg).

2.2. Preparation of modified electrodes

The PPy and NfPPy films were prepared by electropolymerization of pyrrole (0.1 M) on PGE by applying two, five, and 10 cycles between 0.00 and 0.80 V. A solution of 0.1 M $LiClO_4$, and a mixture of 0.1 M $LiClO_4$ + 0.1 M Na_2CO_3 were used as supporting electrolytes for PPy and NfPPy, respectively. The prepared electrodes were rinsed with double distilled water, thereafter maintained in 10% $HClO_4$ solution for 24 h to remove the carbonate ions as carbon dioxide [26, 34]. The PPy was overoxidized by successive potential scans by applying two, five, and 10 cycles between +0.00 and +0.90 V in 0.1 M NaOH. It was then conditioned by performing DPV measurements of DA between 0.00 and +0.6 V. The results showed that the best response to determination of DA was obtained at the polymer film thickness by the application of five cycles, and PPy overoxidation by the application of 10 cycles in a mixture of 0.1 M $LiClO_4$ + 0.1 M Na_2CO_3 (hereafter referred to as $OO_{10}NfPPy_5PGE$). The MEs were coded as OO_aNfPPy_bPGE, where ‘‘a’’ was the number of cycles for over oxidation and ‘‘b’’ was the number of cycles for polymerization of pyrrole on the PGE. All of the prepared electrodes were maintained at room temperature in a desiccator until use.

2.3. Preparation of real samples

The real samples containing DA were used to show the analytical performance of the sensor. The DA HCl was purchased from a local pharmacy, and the solution was transferred to the voltammetric cell for analysis. The standard additions method was employed to reduce the matrix effect in the direct analysis of the pharmaceutical sample. Human serum samples were obtained from three healthy and non-smoking volunteers (V1: female, 54 years, V2: female, 28 years and V3: male, 57 years). The solutions were added into a voltammetric cell to be analyzed without any further

treatment. The standard addition method was used for the determination of the DA. The serum samples were centrifuged, and then after filtering diluted with phosphate buffer solution (pH 4) without any further treatment.

2.4. Electrochemical impedance spectroscopy measurement

Electrochemical impedance measurements were performed with a conventional three-electrode system. In all electrochemical experiments, an Ag/AgCl electrode, Pt wire and PGE with a 0.1 cm^2 geometrical surface area, were used as a reference, counter and working electrode, respectively. Electrochemical impedance spectra of the electrodes were provided at open circuit potential over a 10^5–10^{-2} Hz frequency range at an amplitude of 10 mV. The spectra were fitted with an equivalent circuit model, as shown in Fig. 6.b and Fig. 6.c. All of the electrochemical impedance experiments were conducted using a Gamry 3000 model Potantiostat-Galvanostat system.

3. RESULTS AND DISCUSSION

3.1. Cyclic voltammetry

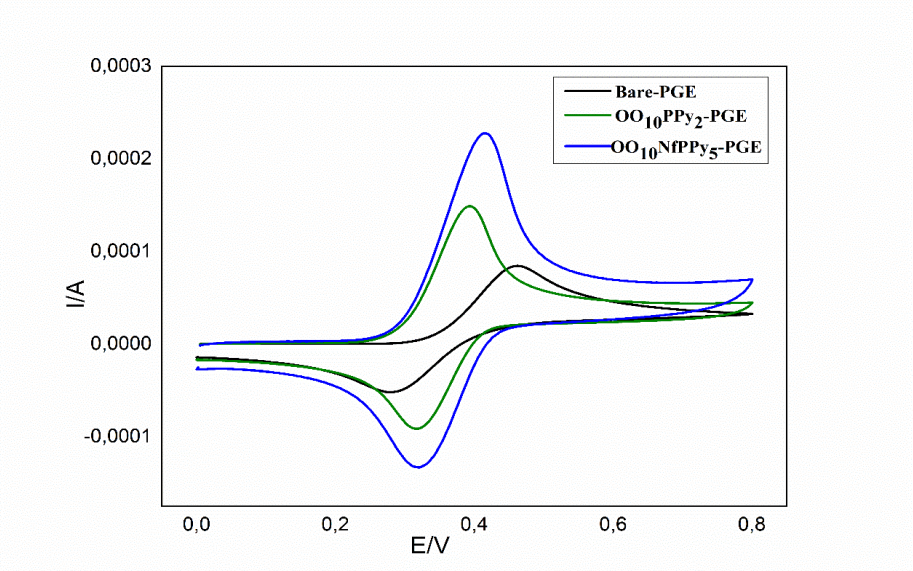

Figure 2. Cyclic voltammograms of dopamine with bare-PGE (black), $OO_{10}PPy_2PGE$ (green), and $OO_{10}NfPPy_5PGE$ (blue) (10^{-3} M dopamine, scan rate: 100 mV/s).

The electrochemical response of a solution having homogeneous DA (10^{-3} M) was determined by cyclic voltammetry with a scan rate of 100 mV s^{-1} under optimized parameters using $OO_{10}NfPPy_5PGE$. An anodic and a cathodic peaks were observed for the oxidation and reduction of

DA at 0.41 and 0.32 V, respectively, using $OO_{10}NfPPy_5PGE$. One oxidation and one reduction peaks were observed at the peak potentials of 0.46 and 0.28 V for DA with bare-PGE, as shown in Fig. 2.

The potential difference (ΔE) between the anodic and cathodic peaks was calculated as being 0.09 and 0.18 V for $OO_{10}NfPPy_5PGE$ and bare-PGE, respectively. The cathodic and anodic peak potentials approach each other with the modification process, that is, decreasing of ΔE value shows that redox reactions happen faster and easier. In addition, the peak current intensity increased with increasing of the electron transfer performance [35, 36]. The cyclic voltammograms of DA at different PGEs are given in Table 1. These data show that the modified electrode (ME) surface behaves differently from a bare-PG electrode. Furthermore, when modified electrode and bare electrode were compared, higher peak currents and reversible voltammograms were obtained with modified electrode. All of these results indicate that the modified electrode can be used for analysis of DA.

Table 1. The oxidation and reduction properties of DA at modified and unmodified PGEs.

Electrode	Peak height of oxidation peak (A)	Peak height of reduction peak (A)	Peak area of oxidation peak (cm^2)	Peak area of reduction peak (cm^2)
Bare-PGE	$7.28x10^{-5}$	$-5.88x10^{-5}$	$1.35x10^{-5}$	$1.09x10^{-5}$
$OO_{10}PPy_2PGE$	$13.5x10^{-5}$	$-10.1x10^{-5}$	$1.91x10^{-5}$	$1.49x10^{-5}$
$OO_{10}NfPPy_5PGE$	$20.2\ x10^{-5}$	$-13.8\ x10^{-5}$	$2.92x10^{-5}$	$2.12x10^{-5}$

3.2. Effect of scan rate

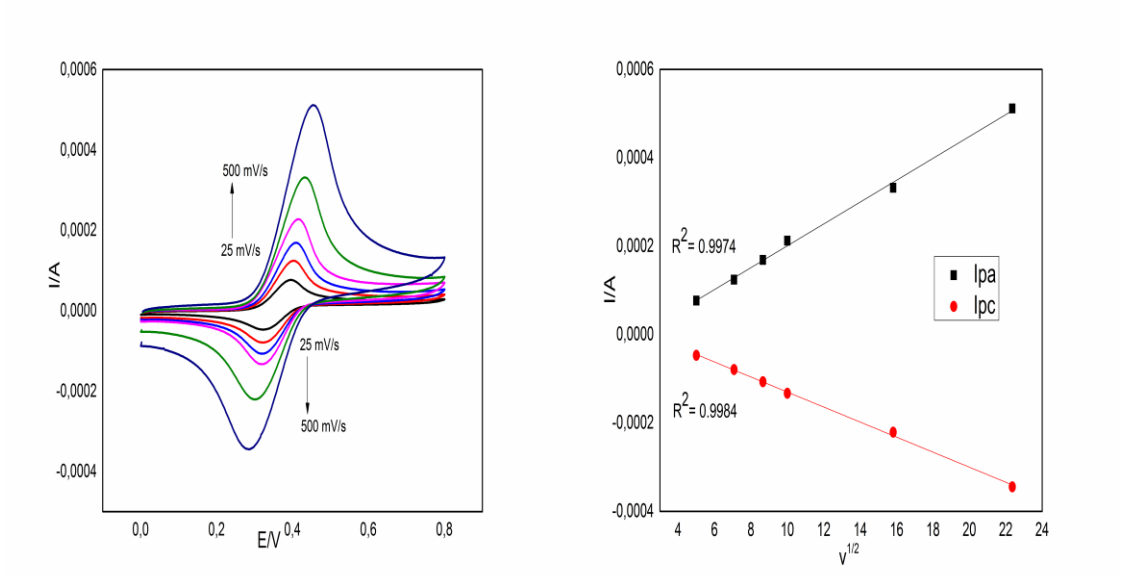

Figure 3. Cyclic voltammograms of DA taken at different scan rates (left) and the graph of the square root of scan rates versus anodic and cathodic peak currents (right).

Useful information involving electrochemical mechanism generally can be acquired from the relationship between peak current and square root of scan rate. Therefore, cyclic voltammograms were taken for DA at different scan rates between 25 and 500 mV/s. A linear relationship between the peak current (Ip) (Ip_a is anodic peak current (R^2=0.9974) and Ip_c is cathodic peak current (R^2=0.9984)) and the square root of scan rate ($\nu^{1/2}$), was also observed, which indicates that the existence of a typical diffusion-controlled mechanism prevail for DA, with electrochemical reactions at different scan rates (Fig. 3) [37, 38].

3.3. pH studies

The pH of the solution is important for the determination of DA, and its effect on the performance of the $OO_{10}NfPPy_5PG$ electrode was investigated at a range of different pH concentrations, from 3 to 9. The response of the $OO_{10}NfPPy_5PG$ electrode to DA (1 μM) at these different pH values is shown in Fig. 4. The DA gave one well-defined anodic peak at $OO_{10}NfPPy_5PGE$. The maximum peak current response was obtained at a pH of 4, with phosphate buffer solution (PBS), giving an oxidation peak at 0.361 V. At pH 4 DA (pKa=8.87) exits in cationic form, while AA (pKa=4.17) can be found almost equally in cationic as well as anionic forms. Even the concentration of AA was 25 times larger than that of DA, much smaller detected peak of AA, compared to that of DA, clearly demonstrated that pH of 4 is a good choice, although it not compatible with physiological pH. (Fig. 10) [39, 40].

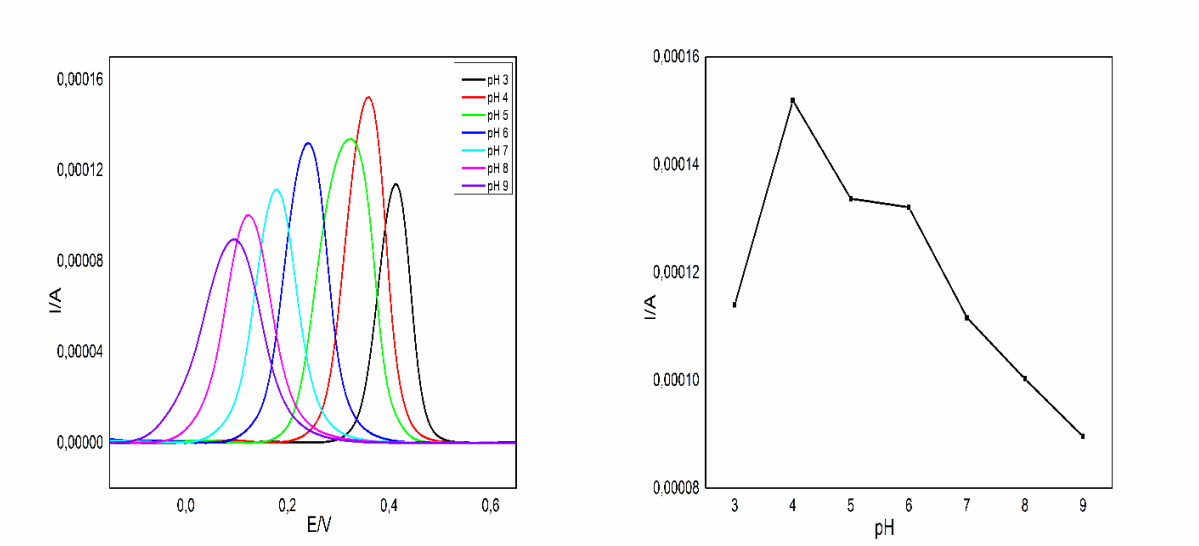

Figure 4. Differential pulse voltammograms of 1 μM dopamine at different pH with $OO_{10}NfPPy_5PGE$ (left) and the relationship between the peak current and the pH (right).

In addition, DPV measurement of dopamine was taken at pH 7.4 to demonstrate the applicability of the electrode at physiological pH (Fig. 5). Moreover, in terms of purely electrostatic interaction, the permselective PPy cannot exclude UA (pKa=5.4). Therefore, pH 4 was selected as the

optimal pH value of the solution, and this medium was further used for the measurement of calibration dependences.

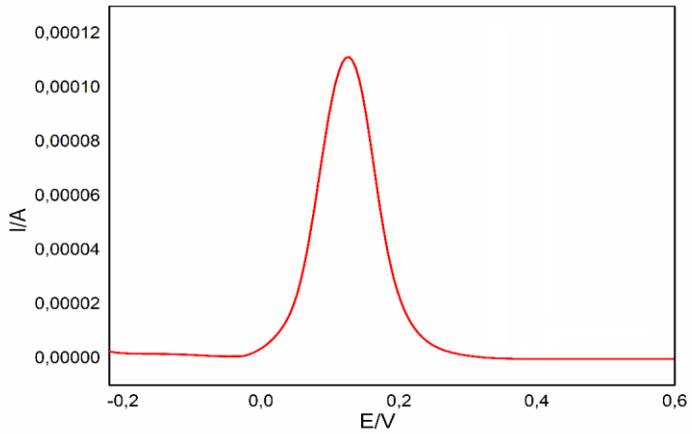

Figure 5. Differential pulse voltammogram of 10^{-3} M dopamine at pH 7.4 with $OO_{10}NfPPy_5PGE$ electrode (scan rate: 100 mV/s, reference electrode: Ag/AgCl).

3.4. Evaluation of electroactive surface area

The electroactive surface areas of the PGE and $OO_{10}NfPPy_5PGE$ were calculated using Randles-Sevcik equation (1). The peak current values (Ip) in this equation were obtained from cyclic voltammograms taken at different scan rates in a 0.1 mol L^{-1} KCl + 1.0 mmol L^{-1} $K_4Fe(CN)_6$ solution [41]. There is a linear relationship between Ip and scan rate ($\nu^{1/2}$) according to Randles-Sevcik equation.

$$Ip = (2.69x10^{-5})\, n^{1/2}\, AD^{1/2}\, C^{*}\nu^{1/2} \quad (1)$$

In this equation, *n* is the number of electrons participating in the redox reaction, *A* is the area of the electrode (cm^2), *D* is the diffusion coefficient of the molecules in the solution (cm^2/s), *C** is the concentration of the probe molecule in the bulk solution (mol cm^{-3}), *v* is the scan rate of the potential perturbation (V/s), and *Ip* is the peak current of the redox couple. In the equation, the effective surface area (A) can be calculated from the value of $\dot{I}p / v^{1/2}$ since D, n (n = 1), and *C** (1.0 mmol L^{-1}) are constant values. The diffusion constant value at 25 °C (D= 6.7 × 10^{-5} cm^2 s^{-1}) was supplied from the literature [41, 42]. The Ip value is increased by increasing the square root of the scanning rate which indicates that the reactions on the ME's surface were reversible. The electroactive areas of the PGE and $OO_{10}NfPPy_5PGE$ were calculated as 4.54 x 10^{-8} cm^2 and 1.05 x 10^{-6} cm^2, respectively. Obviously, when the bare-PGE surface was modified, the electroactive surface area increased about 400 times. As a result, the sensor ($OO_{10}NfPPy_5PGE$) was found to be much more sensitive to DA.

3.5. Comparison of modified electrodes and calibration curve

The polymer film thickness on the electrode surface is an important factor affecting the performance of the electrode for determination of DA. To find the optimum PPy film thickness,

electrochemical polymerizations of pyrrole were carried out at different number of cycles at the potential range between 0.00 and +0.6 V. The maximum peak current value was obtained for the oxidation of DA by applying 5 cycles in the electrochemical polymerization (Fig. 6). The number of optimum cycles for overoxidation of PPy is 10 cycles in 0.1 M $LiClO_4$ + 0.1 M Na_2CO_3 (Fig. 6).

Herein, the peak potential shifts were observed in a different modification processes. This shows that the modification process was successfully performed. The results showed that the performance of all of the synthesized electrodes was better than the performance of the bare electrode.

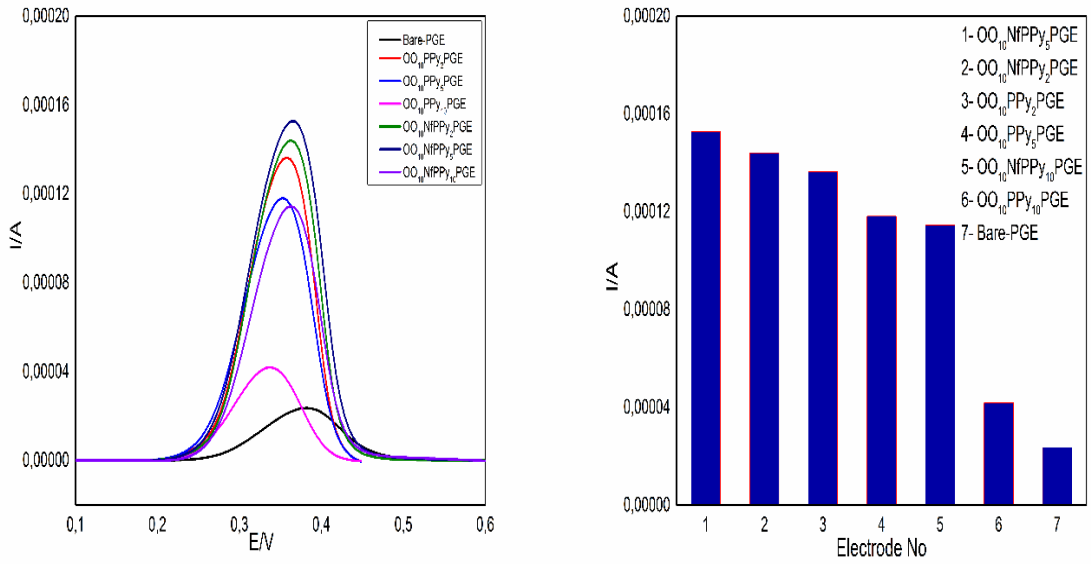

Figure 6. Differential pulse voltammograms of 10^{-3} M DA in phosphate buffer solution (pH: 4) obtained by modified electrodes prepared in different cycle numbers (left). Peak current values obtained from the modified electrodes prepared in different cycle numbers (right).

The mass transfer type is diffusion in the electrochemical determination of dopamine. Therefore, the more the surface area of the electrode, the more the amount of DA that is diffused on the electrode surface, thus smaller concentrations of DA can be determined. In the present study, we used NfPPy film in order to expand the surface area of the cheap graphite electrode as much as possible. However, there are two main reasons for the overoxidation process. First, conductive polymers have large reduction and oxidation peaks because they are electroactive. These peaks are likely to overlap with the analyte peaks. When the conductive polymer is overoxidized, it loses its conductivity, hence its electro activity considerably decreases, thereby minimizing the likelihood of interference with the analyte. When DA is oxidized, the analyte loses electrons and becomes a cationic (positively charged) structure.

The electrode must have the opposite charge, that is, a negative charge, to electrostatically hold the DA at the surface. Carbonyl, carboxyl, hydroxyl, and hydroquinone functional groups (negative polarity) that form at the electrode surface during overoxidation reduce overvoltage of the electrode [43]. Oxygen groups formed on the electrode surface interact with numerous organic and inorganic substances, leading to electron exchange, hydrogen bonding, and electrostatic attraction [22]. Graphite

(main material of the electrode) and NfPPy film with a large surface area are carbon-based, and the amount of functional groups containing oxygen on the surface is increased when the overoxidation process is applied. As this number increases, the selectivity of the electrode to positively charged DA increases. Thus, the electrocatalytic effect and selectivity of the OONfPPyPGE for the DA is improved.

Fig. 7 shows the differential pulse voltammograms recorded on the $OO_{10}NfPPy_5PGE$ in the various concentrations of DA. A linear response was observed in the range of 1.0 and 1000 μmol L^{-1} (R^2 = 0.9986). All experiments performed to estimate the sensitivity of the method for low initial concentration range were repeated 10 times and the standard deviation was calculated. The limit of detection (LOD) was 0.00695 μM DA, via the equation of LOD = $3S_b/m$, where S_b is the standard deviation of the blank response and m is the slope of the calibration plot. In this study, the preparation of the sensor in a few steps and in a short time was an important advantage. Moreover, the abundant availability and low cost of the sensor were also advantageous. Table 2 shows a comparison of some experiments with different electrodes for the determination of DA.

Table 2. A comparison of some studies related to the different electrodes used for the determination of dopamine.

Electrode	Method	Linear range (μmol L^{-1}) for DA	Detection limit (μmol L^{-1}) for DA	Ref.
PPy/eRGO-modified electrode	DPV	0.1-150	0.023	[44]
PPy/SWCNTs/DM/GCE	SWV	0.02-100.000	0.003	[45]
PPy-CNT-GC electrode	DPV	1.000-100.000	0.1	[46]
PPyoxd/SWNTs/GCE	DPV	1.000-50.000	0.38	[47]
PPy-CR-GCE	DPV	0.5-100	0.1	[48]
PPy-RGO	DPV	0.01-10	0.001	[49]
PPyox/AZ/Au	DPV	0.1-30	0.05	[50]
$OO_{10}NfPPy_5PGE$	DPV	1-1000	0.00695	Present work

Abbreviations: DPV differential pulse voltammetry; SWV square wave voltammetry; GCE glassy carbon electrode; MWNT: multiwalled nanotube; MWCNT: multiwalled carbon nanotube; SWCNT: singlewalled carbon nanotube; eRGO: electrochemically reduced graphene oxide; RGO: reduced graphene oxide; CR: congo red; DM: dodecylamine; AZ: aszophloxine.

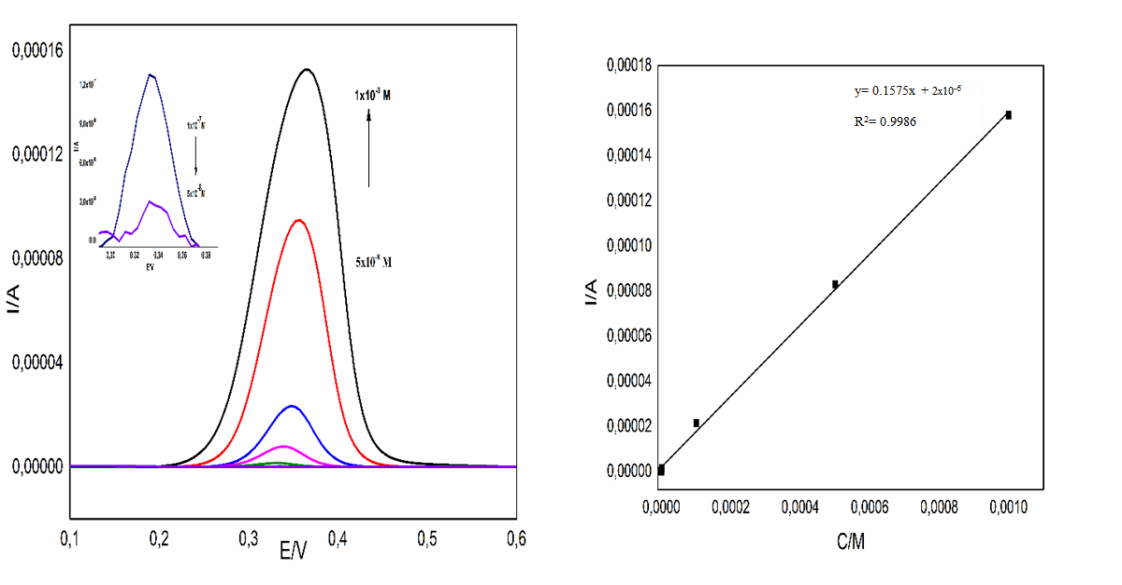

Figure 7. Differential pulse voltammograms obtained at $OO_{10}NfPPy_5PGE$ for different concentrations of dopamine (DA) in phosphate buffer solution (pH4) (insets: calibration curves of the $OO_{10}NfPPy_5PGE$ as a function of DA concentrations).

3.6. Electrochemical impedance spectroscopy

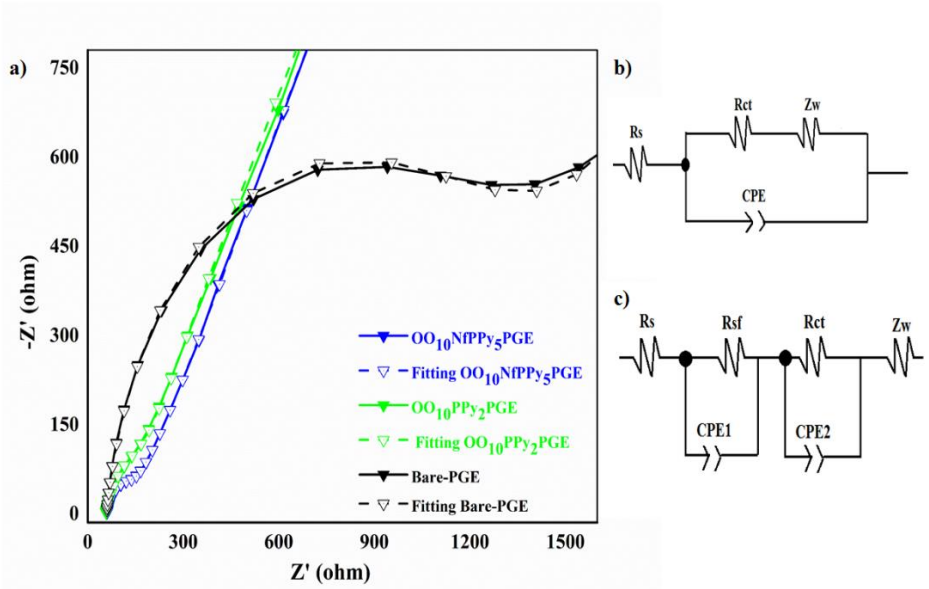

Figure 8. a) Nyquist diagrams of $OO_{10}NfPPy_5$, $OO_{10}PPy_2PGE$, and bare-PGE in electrolytes consisting of 10^{-3} M dopamine in pH4 phosphate buffer solution and **b)** used the equivalent circuit model for bare-PGE fitting of spectra **c)** used the equivalent circuit model for $OO_{10}NfPPy_5PGE$ and $OO_{10}PPy_2PGE$ fitting of spectra.

The EIS can provide useful information about impedance changes of the electrode surface to characterize the phased construction process of the ME. The capacity of electron transfer of bare-PGE, $OO_{10}NfPPy_5PGE$ and $OO_{10}PPy_2PGE$ electrodes was also examined using EIS, as shown in Fig. 8, and EIS was also used to examine the electrode surface coating of PPy film. Nyquist diagrams of

$OO_{10}NfPPy_5PGE$, $OO_{10}PPy_2PGE$, and bare-PGE were carried out with 10^{-3}M DA in pH4 PBS at room temperature (Fig. 8a). The spectra were fitted to a known equivalent circuit model, which is shown in Fig. 8b and Fig. 8c, as comprehensively reported in previous studies [51, 52].

Rs, Rct, Zw, Zphz, CPE1, CPE2, and R_{sf} represent solution resistance, charge transfer resistance, Warburg impedance, phase angle, a constant phase element of the electrode/solution interface and a constant phase element for PPy, NfPPy coating and surface film resistance, respectively [51-53]. The higher electrocatalytic behavior of $OO_{10}NfPPy_5PGE$ was confirmed by the reduction of the charge transfer resistance in electrochemical impedance spectra. By fitting the data using an appropriate equivalent circuit, the values of charge transfer resistance were determined and found to be 1235, 59.04, 51.04 bare-PGE, $OO_{10}PPy_2PGE$, and $OO_{10}NfPPy_5PGE$.modified electrodes, respectively (Table 3). Moreover, $OO_{10}NfPPy_5PGE$ showed the lowest Rsf and Rct, and the highest CPE1, CPE2, Zw and Zphz values. According to these results the $OO_{10}NfPPy_5$ electrode had the highest electron transfer rate and capacities, and the highest sensitivity to DA.

Table 3. Phase angles and fitting results for electrochemical impedance spectroscopy measurements of $OO_{10}NfPPy_5$, $OO_{10}PPy_2PGE$, and Bare-PGE in 10^{-3} M DA pH 4 phosphate buffer solution.

Electrode	Rs (Ω)	Rct (Ω)	CPE2 (F)	Rsf (Ω)	CPE1 (F)	Zw	Zphz (^{o})
$OO_{10}NfPPy_5$ PGE	57.18	51.04	$2.18x10^{-5}$	$1.679x10^{3}$	$1.81x10^{-3}$	$3.891x10^{-3}$	51.39
$OO_{10}PPy_2$ PGE	55.19	59.04	$32.24x10^{-6}$	$22.17x10^{3}$	$1.90x10^{-4}$	$3.761x10^{-3}$	49.54
Bare-PGE	58.99	1235	$2.91x10^{-6}$	-	-	$27.7x10^{-5}$	23.75

Abbreviations: Rs: solution resistance; Rct: charge transfer resistance; CPE: constant phase element; Rsf: surface film resistance; Zw: Warburg impedance; Zphz: phase angle.

3.7. Surface morphology

The surface images of the PPy films were investigated using a SEM. The structure of PPy films obtained by electropolymerization method depends on the counter-ion, solvent, and polymerization medium. The surface image of the electrode before any modification process is shown in Fig. 9a. The counter-ion in an aqueous media was obtained on the electrode surface only when used with spherical morphology; the $LiClO_4$ PPy "cauliflowers" structure is similar (Fig. 9b) [24]. In contrast, when $LiClO_4$ was used with Na_2CO_3 in the solution medium, the nanofiber structure of PPy was observed (Fig. 9c and Fig. 9d). Links between these fibers led to a remarkable improvement of the current, thus the reticulated polymeric network formed a surface area. In this case, the electrode became more sensitive for DA.

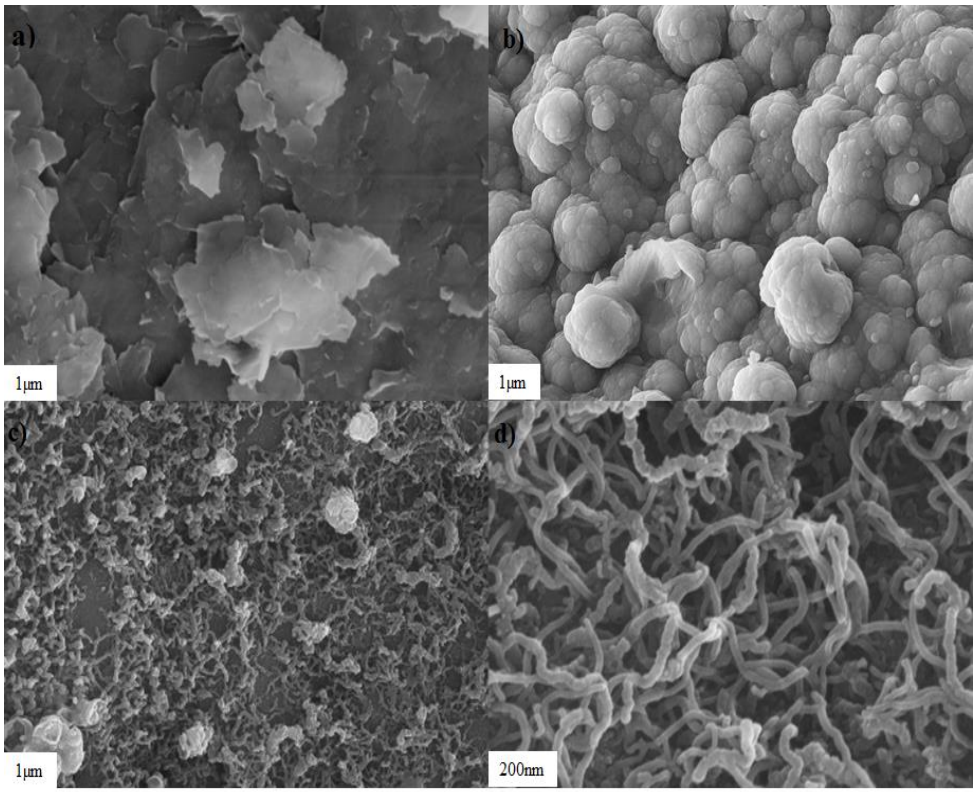

Figure 9. Scanning electron microscope images of **a**) bare-PGE, **b)** $OO_{10}PPy_2PGE$, **c)** and **d)** $OO_{10}NfPPy_5PGE$.

3.8. Interferences

$OO_{10}NfPPy_5PGE$ selectivity was identified in the presence of various interfering species. The electrode was more electroactive in PBS (pH4) (as shown in Fig.4), and the voltammetric response in the presence of interfering species, such as UA and AA, was examined, as these three substances are very generally found together [54, 55]. The oxidation peak of AA frequently overlaps with that of DA on solid electrodes. On the other hand, UA has individual oxidation potential but its existence mainly affects the adsorption properties and electrochemical oxidation of DA [56]. Therefore, a 0.1 mM concentration of 25 times as much AA (2.5 mM) and about five times as much UA (0.415 mM) was added to the DA solution, and the responses of the electrodes were investigated via the DPV method (Fig. 10). As shown in Fig. 10, the AA and UA show interference effects, when bare-PGE and $OO_{10}PGE$ electrodes was used. However, effect of interference was removed with $OO_{10}PPy_2PGE$ and $OO_{10}NfPPy_5PGE$ electrodes. In addition to, while $OO_{10}NfPPy_5PGE$ was less selective for UA, it was more selective for DA. As mentioned in the pH study section, $OO_{10}NfPPy_5PGE$ was distinguished dopamine from other species even in high concentrations of other species (AA and UA). All of these results showed that simultaneous determination of these three substances with $OO_{10}NfPPy_5PGE$ can be successfully done.

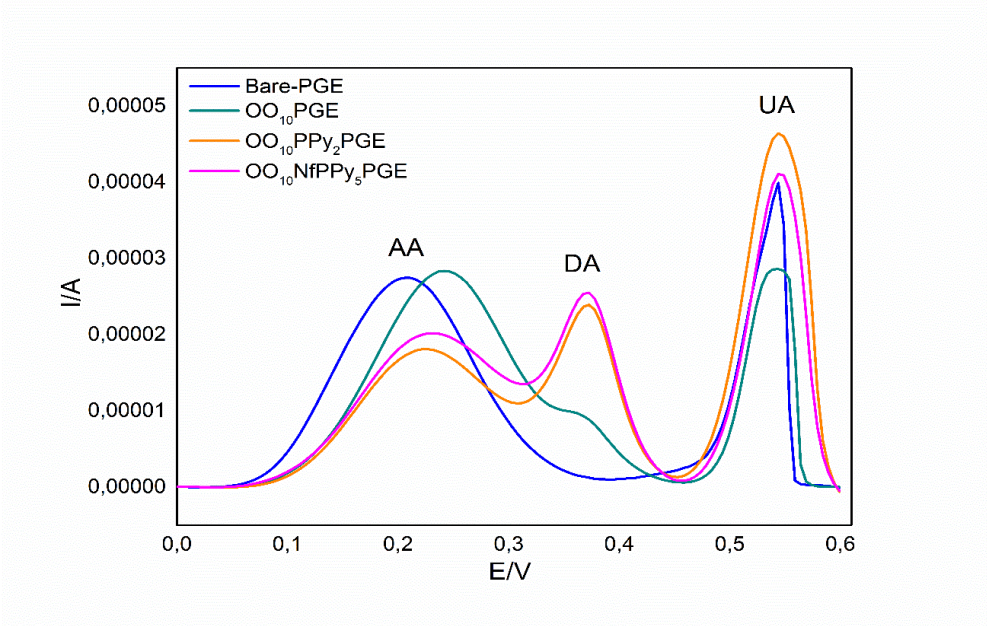

Figure 10. A combination of 2.5 mM AA, 0.1 mM DA, and 0.415 mM UA with bare-PGE, $OO_{10}PGE$, $OO_{10}PPy_2PGE$, and $OO_{10}NfPPy_5PGE$ electrodes' differential pulse voltammograms (pH 4 phosphate buffer solution).

3.9. Real samples analysis

Table 4. A real sample analysis performed using high-performance liquid chromatography and $OO_{10}NfPPy_5PGE$ electrode.

Real sample name	Reported DA content (mg/mL)	Detected DA (mg/mL) with $OO_{10}NfPPy_5PGE$	RSD (%) (n=3)	Detected DA reference method with HPLC	RSD (%) (n=3)
Dopamine HCl ampul	40.0[a]	40.72[a]	1.13	40.38[a]	0.74

[a] mg/mL.

The real sample was diluted 100 times with PBS (pH 4) without any further treatment. The solution was then added into the voltammetric cell for analysis. The standard additions method was employed to reduce the matrix effect in a direct analysis of real samples. Then, DPV measurements were carried out. It was found that the value specified by the drug manufacturers was fairly compatible with the amount of DA obtained in studies performed with the voltammetric prepared electrode. The results obtained by the DPV method for validity of the electrochemical methods used in the analysis were compared with results obtained by HPLC analysis. Chromatographic measurements were made

by HPLC system with gradient pump and UV-Vis detector. (Mobile phase: 0.005 M sodium-1-octane sulphonate and acetonitrile (87:13), (test solution: 16 mg (1 mmol / Sample solution corresponding to dopamine HCl and mobile diluted to 100 mL). The HPLC analysis and DPV values were obtained by the manufacturer with the value reported by the company (Table 4). The results obtained by both methods were compatible with each other and both methods can be used for analytical purposes.

The usability of the mentioned sensor was tried with the assay of the DA content of human serum samples. The recoveries were detected by spiking the samples with an enough amount of standard solutions of DA, and the results were identifying to be 94.8-102.7%. Therefore, this method could be applied to DA determination in human serum samples with remarkable results. In human blood serum, the presence of UA and some other interfering substances, such as proteins and glucose do not interfere with the determination of DA. The satisfactory results are shown in Table 5. The results showed that the proposed method could be used as an easy approach for direct analysis of the real samples.

Table 5. Results for DA determination ($x10^{-5}$mol L^{-1}) in various human serum samples obtained by the proposed method under the optimum conditions with $OO_{10}NfPPy_5PGE$ electrode.

Real sample name	Added ($x10^{-5}$mol L^{-1})	Found ($x10^{-5}$ mol L^{-1})	Recovery (%)
V1	2.0	1.90	97.4
V2	2.0	1.87	96.4
V3	2.0	1.92	98.1
Mean		1.90	97.3

3.10. Reproducibility and stability of electrodes

$OO_{10}NfPPy_5PGE$ was investigated for reproducibility of $1.0x10^{-4}$ M DA. Therefore, seven electrodes were prepared and produced under the same conditions, and the peak current values of DPV obtained were compared to DA. It was determined that the oxidation peak intensities of DA had a relative standard deviation of 1.1%. This showed that the $OO_{10}NfPPy_5PGE$ electrodes are reproducible. These electrodes were stored at room temperature and the long-term stability was tested for 60 days. The results showed that the electrode response did not change at the end of this time. It is possible to say that, the $OO_{10}NfPPy_5PGE$ is relatively stable for the determination of DA.

4. CONCLUSIONS

In this study, PPy film modified PGE, as used as a sensor for the determination of DA, was investigated. The use of disposable pencil graphite electrodes meant that the electrode pollution caused by the oxidation of DA and other substances was eliminated. Also, advantage is that the pencil graphite electrode reduces the analysis cost and shortens the analysis time by removing the electrode

cleaning step. Moreover, the sensor was excellent sensitive and selective to DA without the interference in the presence of UA and AA. Furthermore, while the peak currents and electron transfer capacities of anodic and cathodic peaks increased with the use of $OO_{10}NfPPy_5PGE$, the charge transfer resistance decreased. In addition to, the electroactive surface areas of the Bare-PGE and $OO_{10}NfPPy_5PGE$ were also calculated in this study. When all these results are evaluated, the use of $OO_{10}NfPPy_5PGE$ introduced solutions to problems encountered in the electrochemical detection of DA. As a result, the sensor developed for real samples could be effectively used in the determination of DA in the future studies.

ACKNOWLEDGEMENT
This work is financially supported by The Scientific & Technological Research Council of Turkey (TUBITAK) (Project No: 113Z905).

References

1. M.L. Heien, A.S. Khan, J.L. Ariansen, J.F. Cheer, P.E. Phillips, K.M. Wassum, R.M. Wightman, *Proc. Natl. Acad. Sci. U S A*, 102 (2005) 10023.
2. S.S. Castro, R.J. Mortimer, M.F. De Oliveira, N.R. Stradiotto, *Sensors*, 8 (2008) 1950.
3. A.A. Grace, *Neuropharmacology*, 62 (2012) 1342.
4. L. Guo, Y. Zhang, Q. Li, *Anal. Sci.*, 25 (2009) 1451.
5. K. Vuorensola, H. Sirén, U. Karjalainen, *J. Chromatogr. B*, 788 (2003) 277.
6. C.A. Heidbreder, L. Lacroix, A.R. Atkins, A.J. Organ, S. Murray, A. West, A.J. Shah, *J. Neurosci. Methods*, 112 (2001) 135.
7. P.S. Rao, N. Rujikarn, J. Luber Jr, D. Tyras, *Chromatographia*, 28 (1989) 307.
8. J.-L. Chen, X.-P. Yan, K. Meng, S.-F. Wang, *Anal. Chem.*, 83 (2011) 8787.
9. J. Li, N. Zhang, Q. Sun, Z. Bai, J. Zheng, *Talanta*, 159 (2016) 379.
10. J.-W. Oh, Y.W. Yoon, J. Heo, J. Yu, H. Kim, T.H. Kim, *Talanta*, 147 (2016) 453.
11. J.-W. Mo, B. Ogorevc, *Anal. Chem.*, 73 (2001) 1196.
12. F. Cruz Moraes, M.F. Cabral, S.A. Machado, L.H. Mascaro, *Electroanalysis*, 20 (2008) 851.
13. Z. Hua, Q. Qin, X. Bai, C. Wang, X. Huang, *Sens. Actuators, B*, 220 (2015) 1169.
14. H. Xu, J. Xiao, L. Yan, L. Zhu, B. Liu, *J. Electroanal. Chem.*, 779 (2016) 92.
15. S. Bahrami, A.R. Abbasi, M. Roushani, Z. Derikvand, A. Azadbakht, *Talanta*, 159 (2016) 307.
16. H. Zhao, Y. Zhang, Z. Yuan, *Anal. Chim. Acta*, 441 (2001) 117.
17. H. Yao, Y. Sun, X. Lin, Y. Tang, L. Huang, *Electrochim. Acta*, 52 (2007) 6165.
18. X. Kan, H. Zhou, C. Li, A. Zhu, Z. Xing, Z. Zhao, *Electrochim. Acta*, 63 (2012) 69.
19. C. Wang, P. Xu, K. Zhuo, *Electroanalysis*, 26 (2014) 191.
20. Z. Yang, X. Liu, Y. Wu, C. Zhang, *Sens. Actuators, B*, 212 (2015) 457.
21. B. Rezaei, M.K. Boroujeni, A.A. Ensafi, *Biosens. Bioelectron.*, 66 (2015) 490.
22. J. Li, J. Zhao, X. Wei, *Sens. Actuators, B*, 140 (2009) 663.
23. A. Ramanavičius, A. Ramanavičienė, A. Malinauskas, *Electrochim. Acta*, 51 (2006) 6025.
24. A. Özcan, Y. Şahin, M. Özsöz, S. Turan, *Electroanalysis*, 19 (2007) 2208.
25. L. Özcan, Y. Şahin, *Sens. Actuators, B*, 127 (2007) 362.
26. L. Özcan, Y. Şahin, H. Türk, *Biosens. Bioelectron.*, 24 (2008) 512.
27. Z. Gao, Z. Minxian, C. Beshen, *J. Electroanal. Chem.*, 373 (1994) 141.
28. A.M. Farrington, J.M. Slater, *Electroanalysis*, 9 (1997) 843.
29. L.D. Spurlock, A. Jaramillo, A. Praserthdam, J. Lewis, A. Brajter-Toth, *Anal. Chim. Acta*, 336 (1996) 37.

30. H. Shiigi, M. Kishimoto, H. Yakabe, B. Deore, T. Nagaoka, *Anal. Sci.*, 18 (2002) 41.
31. M. Ishifune, R. Suzuki, Y. Mima, K. Uchida, N. Yamashita, S. Kashimura, *Electrochim. Acta*, 51 (2005) 14.
32. H. Görçay, G. Türkoğlu, Y. Şahin, H. Berber, *IEEE Sens. J.*, 14 (2014) 2529.
33. H. Görçay, İ. Çelik, E. Yurdakul, Y. Şahin, Ş. Kökten, *IEEE Sens. J.*, 16 (2016) 2914.
34. Y. Tian, J. Wang, Z. Wang, S. Wang, *Synth. Met.*, 143 (2004) 309.
35. O.Gilbert, B.E.K. Swamy, *J. Electroanal. Chem.*, 636 (2009) 80.
36. L. Yang, D. Liu, J. Huang, T. You, *Sens. Actuators, B*, 193 (2014) 166.
37. U. Chandra, B.E.K. Swamy, O. Gilbert, S.S. Shankar, K.R. Mahanthesha, B.S. Sherigara, *Int. J. Electrochem. Sci.*, 5 (2010) 1.
38. H. Zhao, Y. Zhang, Z. Yuan, *Analyst*, 126 (2001) 358.
39. D.P. Quan, D.P. Tuyen, T.D. Lam, P.T.N. Tram, N.H. Binh, P.H. Viet, *Colloids Surf., B*, 88 (2011) 764.
40. T.E.M. Nancy, V.A. Kumary, *Electrochim. Acta*, 133 (2014) 233.
41. Ş.U. Karabiberoğlu, Z. Dursun, *J. Solid State Electrochem.*, (2016) 1.
42. S. Konopka, B. McDuffie, *Anal. Chem.*, 42 (1970) 1741.
43. R.C. Engstrom, *Anal. Chem.*, 54 (1982) 2310.
44. P. Si, H. Chen, P. Kannan, D.-H. Kim, *Analyst*, 136 (2011) 5134.
45. J. Li, Y. Liu, W. Wei, S. Luo, *Anal. Lett.*, 44 (2011) 1226.
46. S. Shahrokhian, E. Asadian, *J. Electroanal. Chem.*, 636 (2009) 40.
47. Y. Li, P. Wang, L. Wang, X. Lin, *Biosens. Bioelectron.*, 22 (2007) 3120.
48. S. Shahrokhian, H.R. Zare-Mehrjardi, *Electroanalysis*, 21 (2009) 157.
49. T. Qian, S. Wu, J. Shen, *Chem. Commun.*, 49 (2013) 4610.
50. M.B. Gholivand, M. Amiri, *J. Electroanal. Chem.*, 676 (2012) 53.
51. J. Cao, G. Hu, Z. Peng, K. Du, Y. Cao, *J. Power Sources*, 281 (2015) 49.
52. A. El Jaouhari, M. Laabd, E. Bazzaoui, A. Albourine, J. Martins, R. Wang, G. Nagy, M. Bazzaoui, *Synth. Met.*, 209 (2015) 11.
53. N.F. Atta, A. Galal, S.M. Ali, S.H. Hassan, *Ionics*, 21 (2015) 2371.
54. A.M. Granero, G.D. Pierini, S.N. Robledo, M.S. Di Neizo, H. Fernández, M.A. Zon, *Microchem. J.*, 129 (2016) 205.
55. R.N. Goyal, V.K. Gupta, N. Bachheti, R.A. Sharma, *Electroanalysis*, 20 (2008) 757.
56. A.A. Ensafi, M. Taei, T. Khayamian, *Int. J. Electrochem. Sci.*, 5 (2010) 116.